Mouse maternal protein restriction during preimplantation alone permanently alters brain neuron proportion and adult short-term memory

Joanna M. Gould[1,3], Phoebe J. Smith[1], Chris J. Airey[1], Emily J. Mort[2], Lauren E. Airey[1], Frazer D.M. Warricker[1], Jennifer E. Pearson-Farr[2,] Eleanor C. Weston[2,] Philippa J.W. Gould[2], Oliver G. Semmence[2], Katie L. Restall[2], Jennifer A. Watts[2], Patrick C. McHugh[4], Stephanie J. Smith[2,3], Jennifer M. Dewing[1,3], Tom P. Fleming[2,3], Sandrine Willaime-Morawek [1,3,5]

[1] Clinical Neurosciences and Psychiatry, CES, Faculty of Medicine, University of Southampton, Southampton, SO16 6YD, UK;
[2] Biological Sciences, University of Southampton, Southampton, SO16 6YD, UK
[3] Centre for Human Development, Stem Cells and Regeneration, University of Southampton, Southampton, SO16 6YD, UK
[4] Centre for Biomarker Research (CeBioR), University of Huddersfield, Huddersfield | HD1 3DH, UK

[5] Corresponding author:
Sandrine Willaime-Morawek,
Faculty of Medicine, University of Southampton
LD72, South Laboratory Block, Southampton General Hospital, Mailpoint 806
Southampton SO16 6YD, UK
tel: +44 (0)23 8120 6107; fax: +44 (0)23 8120 6085

Author contribution summary:
conception and design: JMG, TPF, SWM
collection and/or assembly of data: JMG, PJS, CJA, EJM,LEA, FDMW, JEPF, ECW, PJWG, OGS, KR, JAE, PCM^{c}H, SJMS, JD
data analysis and interpretation: JMG, PJS, CJA, EJM, LEA, FDMW, JEPF, ECW, PJWG, OGS, KR, JAE, SJMS, JD, TPF, SWM
manuscript writing: TPF, SWM
final approval of manuscript: JMG, PJS, CJA, EJM, LEA, FDMW, JEPF, ECW, PJWG, OGS, KR, JAE, PCM^{c}H, SJMS, JD, TPF, SWM
provision of study material or patients: SJMS, TPF
financial support: TPF, SWM

Classification:	Biological Sciences; Neurosciences
Keywords:	DOHaD, neural stem cells, neurogenesis, low protein diet, maternal diet
Short title:	Maternal diet affects offspring adult memory
Figures and tables:	6 figures and 2 tables
Supplemental materials:	4 figures
Pages:	30
Abstract:	215 words

Significance statement: 118 words

Maternal protein malnutrition during pregnancy and lactation compromises brain development, with lasting consequences for motor and cognitive function. However, the importance of nutrition on early brain development is unknown. We have previously shown maternal low protein diet confined to the preimplantation period (Emb-LPD) in mice with normal nutrition thereafter is sufficient to induce cardiometabolic and locomotor behavioral abnormalities in adult offspring. Here, we report that Emb-LPD and sustained LPD reduce neural stem cells (NSCs) in the fetal brain. Moreover, Emb-LPD causes remaining NSCs to upregulate neuronal differentiation in compensation beyond control levels, increase cortex thickness and neuron ratio leading to adult memory deficits. These data demonstrate poor maternal nutrition from conception adversely affects brain development and adult memory.

Abstract

Maternal protein malnutrition throughout pregnancy and lactation compromises brain development in late gestation and after birth, affecting structural, biochemical and pathway dynamics with lasting consequences for motor and cognitive function. However, the importance of nutrition during the preimplantation period for brain development is unknown. We have previously shown maternal low protein diet confined to the preimplantation period (Emb-LPD) in mice with normal nutrition thereafter is sufficient to induce cardiometabolic and locomotory behavioral abnormalities in adult offspring. Here, we report, using a range of *in vivo* and *in vitro* techniques, that Emb-LPD and sustained LPD reduce neural stem cell (NSCs) and progenitor cell numbers at E12.5, E14.5 and E17.5 through suppressed proliferation rates in both ganglionic eminences and cortex of the fetal brain. Moreover, Emb-LPD causes remaining NSCs to upregulate the neuronal differentiation rate beyond control levels, whereas in LPD, apoptosis increases to possibly temper neuron formation. Furthermore, Emb-LPD adult offspring maintain the increase in neuron proportion in the cortex, display increased cortex thickness and short-term memory deficit analyzed by the novel object recognition assay. Lastly, we identify altered expression of fragile X family genes as a potential molecular mechanism for adverse programming of brain development. Collectively, these data demonstrate poor maternal nutrition from conception is sufficient to cause abnormal brain development and adult memory loss.

\body

Introduction

The concept that *in utero* environment may influence postnatal health and disease risk is now well recognized following the original epidemiological studies on diverse human populations showing low birth weight and early catch-up growth during infancy associated with increased chronic disease in adulthood (1, 2). Such programming consequences also included cognitive decline and other neurodevelopmental disorders (3, 4). The Developmental Origins of Health and Disease (DOHaD) concept has been further supported from human famine datasets, particularly the Dutch Hunger Winter, demonstrating cardiometabolic and neurological dysfunction associate with in utero maternal nutrient depravation during pregnancy (5).

Both human studies and animal models further demonstrate the particular vulnerability of the periconceptional period in DOHaD-related programming. For example, people who were conceived during the Dutch famine (rather than experienced it during later gestation) had increased risk of schizophrenia and depression together with poorer cognitive capacity in later life as well as cardiometabolic consequences (5). Our own mouse studies have shown maternal isocaloric low protein diet fed exclusively during preimplantation development with control diet thereafter and postnatally (Emb-LPD) was sufficient to induce cardiometabolic and behavioral abnormalities in adult offspring (6). Early embryo vulnerability to maternal dietary quality may represent a form of developmental plasticity to coordinate fetal growth and metabolism with prevailing maternal conditions but if conditions change, maladaptation may have consequences for disease risk in adulthood (7).

Animal studies to date show maternal malnutrition during pregnancy and lactation may affect diverse aspects of brain development associated with impaired physical and coordinated movement, hyperactivity, altered social activity and motivation, as well as reduced mental and cognitive function, sometimes in a gender-specific manner (8-10). These consequences may derive from specific detriments on the maturation and functioning of brain tissues such as the hippocampus, cortex and hypothalamus affecting neurotransmitter and hormonal release (11-13). Maternal protein restriction may also affect the proliferation and differentiation capacities

of neural stem cells (NSCs) (14). However, the consequences of maternal protein restriction specifically during early embryonic development on later brain development are unknown.

Here, we compare the effects of maternal Emb-LPD and sustained LPD on mouse brain development and consequences in adult offspring, and show that NSCs proliferation and maintenance are adversely affected by both treatments leading to altered rates of neuronal differentiation. Our study shows maternal dietary quality from conception to be a critical factor in brain developmental capacity with enduring consequences on brain organization and adult behavior.

Results

Maternal protein restriction reduces primary sphere formation from E12.5, E14.5 and E17.5 ganglionic eminences and cortex cells.

We first investigated the effect of maternal low protein diet (fig 1A and table 1) on neurosphere formation (fig 1B), a measure of NSCs and early progenitor potential, from ganglionic eminence and cortex primary cells, at time points around the neurogenesis peak (E12.5-E14.5) in these regions. We observed a significant decrease in the number of neurospheres formed after 7 days in culture, for both LPD and Emb-LPD, compared to NPD at E12.5 (fig 1C,D), E14.5 (fig 1E,F) and E17.5 (fig 1G,H), with a further significant decrease for LPD compared to Emb-LPD in E12.5 ganglionic eminences (fig 1C) and E14.5 ganglionic eminences and cortex cells (fig 1E,F). At E17.5, both the ganglionic eminences and cortex cells from the Emb-LPD group formed significantly fewer neurospheres than both NPD and LPD (fig 1G,H). These results were independent of maternal litter size (multilevel random-effects regression model analysis), the sex of the fetuses (See SI Appendix, fig. S1A) and their position in the uterus. To assess the self-renewal capacity of the neurosphere cells, the primary neurospheres were passaged to give rise to secondary spheres (14 days total culture period from brain dissection). There was no difference in the number of secondary spheres formed from primary neurosphere cells after dissociation (See SI Appendix, fig. S1B). These results reveal that maternal LPD and Emb-LPD caused reduced neurosphere-forming capabilities from ganglionic eminences and cortex primary cells at three fetal ages. This defect is rescued when the cells are passaged and is not present in secondary sphere formation. This suggests that the effect of maternal diet on cell potential does not persist with extended cell culture *in vitro*.

Maternal protein restriction alters the neuronal differentiation pathway in ganglionic eminences and cortex in vivo.

To assess whether the stemness and differentiation status of neural cells was affected by different maternal diets, ganglionic eminences and cortex primary cells were stained for Nestin and Beta-III-tubulin and flow cytometry sorted. The cells analyzed separated into four

main populations: Nestin+ only (Q1, representing NSCs/progenitor cells), double positive cells (Q2, representing neuronal progenitors), Beta-III-tubulin+ only (Q4, representing differentiated neurons), and double negative cells (Q3), compared to isotype control stained cells (fig 2A,B). When closely analyzing the FACS plots (fig 2B), two different populations could be detected in the double positive cell population. These were separated as Nestin+ Beta-III-tubulin dim (representing early neuronal progenitors, Q2N), and Nestin dim Beta-III-tubulin+ (representing late neuronal progenitors Q2B), where dim represent a moderately bright signal compared to the other cell populations (determined by cell density in fig 2B rather than arbitrary gating).

Nestin only positive cells represented only a small percentage of the whole population and showed in ganglionic eminences (fig 2) and cortex (See SI Appendix, fig. S2) cells a significant decrease in Emb-LPD at E12.5, E14.5 and E17.5, as well as in LPD at E12.5 and E14.5, whereas E17.5 LPD Nestin+ only cells did not differ from NPD (fig 2C,G,K and See SI Appendix, fig. S2A,E,I). The decrease in Nestin+ only cells confirms the decrease in sphere-forming cells observed in the sphere assay and suggests a decrease in NSCs at E12.5 and E14.5 in both Emb-LPD and LPD and at E17.5 in Emb-LPD.

Nestin+ Beta-III-tubulin+ cells represented the majority of cells and illustrated the fact that most of the cells were in transition between undifferentiated and neuronally-differentiated cells. When analyzed separately, the two neuronal progenitor populations showed very different results in both ganglionic eminences and cortex at E12.5 and E14.5: the early neuronal progenitors decreased significantly in both Emb-LPD and LPD compared to NPD (fig 2D,H and See SI Appendix, fig. S2B,F) whereas the late neuronal progenitors increased significantly in both Emb-LPD and LPD compared to NPD (fig 2E,I and See SI Appendix, fig. S2C,G). At E17.5, the proportion of both early and late neuronal progenitors in Emb-LPD and early progenitors in LPD was unchanged compared with NPD (fig 2L,M and See SI Appendix, fig. S2J,K) whereas the LPD late progenitor proportion was increased (fig 2M and See SI Appendix, fig. S2K). Beta-III-tubulin only positive cells represent differentiated neurons and showed a significant increase in Emb-LPD E12.5 and E17.5 in both ganglionic eminences and cortex (fig 2F,N and See SI Appendix, fig. S2D,L) with no difference at E14.5 (fig 2J and

See SI Appendix, fig. S2H). In LPD, the Beta-III-tubulin+ cell proportion was significantly increased at E12.5 whereas it was significantly decreased at E14.5 and E17.5 in both ganglionic eminences and cortex (fig 2F,J,N and See SI Appendix, fig. S2D,H,L). Offspring sex effects were not found with statistical analysis in the FACS data at any time points, with 40-50% of the data generated from female offspring.

These detailed FACS analyses are schematically summarized for ganglionic eminences primary cells (fig 3A), with enlargement of the Nestin+ only cells data (fig 3B, light blue). This shows clearly that the proportion of Nestin+ only cells peaks at E14.5 compared to E12.5 and E17.5 in NPD. LPD Nestin+ only cell proportions follow the same pattern across time although at reduced levels at E12.5 and E14.5, whereas the Emb-LPD Nestin+ only cell proportions are low from E12.5 and continuously decrease until E17.5 (fig 3B). Early progenitor (royal blue, Nestin+ Beta-III-tubulin dim cells) proportions decrease at E12.5 and E14.5 in both LPD and Emb-LPD compared to NPD. Late progenitor (purple, Nestin dim Beta-III-tubulin+ cells) proportions increase in Emb-LPD and LPD at both E12.5 and E14.5 as well as in LPD at E17.5, compared to NPD. Differentiated neuron (dark blue, Beta-III-tubulin+ only cells) proportions increase at E12.5 for both Emb-LPD and LPD, as well as at E17.5 for Emb-LPD, whereas they decrease in LPD at both E14.5 and E17.5, compared to NPD. Collectively, in Emb-LPD, there is a reduction in NSCs and an increase in differentiated neurons over time compared with NPD. In LPD, a reduction in NSCs is also evident, but differentiated neuron formation becomes stabilized over time, more similar to NPD.

To confirm these results and to resolve any regional variation within ganglionic eminences and cortex, coronal brain sections were stained for a marker of NSCs Sox2, and a marker of neural progenitors and young neurons, Beta-III-tubulin. Sox2 was chosen, instead of Nestin used in the FACS experiments, as it labels NSCs but not progenitor cells. Staining was quantified in ganglionic eminences ventricular zone (VZ), subventricular zone (SVZ) and mantle zone (MZ), and in cortex in VZ, intermediate zone (IZ) and cortical plate (CP), when relevant. Sox2 staining was present in both the ganglionic eminences and cortex, mostly in the VZ and SVZ/IZ where NSCs reside. Quantification revealed a significant decrease of the

number of positive cells in LPD compared to NPD, in the ganglionic eminences VZ at E12.5 (See SI Appendix, fig. S3A) with a similar trend in the cortex VZ at the same age (See SI Appendix, fig. S3B), as well as in both regions at E14.5 (See SI Appendix, fig. S3 C,D). A similar decreasing trend is noticed in the Emb-LPD group at E12.5 (See SI Appendix, fig. S3A,B) and E14.5 (See SI Appendix, fig. S3C,D). No change is observed at E17.5 (See SI Appendix, fig. S3E,F) in both diet groups and regions, compared to NPD. The decrease in proportion of Sox2+ cells observed here confirms the decrease in NSCs/progenitor cells, seen in the sphere assay and FACS analysis.

Beta-III-tubulin staining was light in VZ of ganglionic eminences, stronger in SVZ and even more in the mantle zone (fig 4A-C). Its quantification showed an increase in Emb-LPD SVZ and MZ in ganglionic eminences at E14.5 (fig 4D) and a comparable trend in the cortex at E14.5 (fig 4E, $p=0.0724$ in IZ and $p=0.0586$ in cortical plate), compared to both NPD and LPD. No difference was found in the VZ (fig 4D,E), as expected as this layer contains mostly undifferentiated cells and very few differentiated neurons. This increase confirms the FACS analysis where collectively the three cell categories positive for Beta-III-tubulin are increased in Emb-LPD at E14.5 (fig 3).

Collectively, these results indicate that maternal diet not only affects the availability of NSCs in the VZ but also their pattern of differentiation towards a neuronal fate in the layers containing more differentiated cells (SVZ, MZ for GE; IZ and CP for cortex). Thus, in Emb-LPD there is a decrease in NSCs/progenitor cells and an increase in late neuronal progenitors and neurons. In contrast, LPD induces a decrease in NSCs/progenitor cells, an increase in late neuronal progenitors but not followed by an increase in neurons.

Maternal protein restriction reduces proliferation of ganglionic eminences and cortex cells.

NSCs need to proliferate to maintain and/or increase their population *in vivo* and to form neurospheres *in vitro*. A defect in proliferation might account for the apparent loss of NSCs seen following Emb-LPD and LPD in the neurosphere, FACS and immunohistochemical

analyses. The growth fraction (Ki67+/DAPI+) was analyzed in the VZ of both cortex and ganglionic eminence coronal sections (fig 5A-C). The growth fraction significantly decreased for both Emb-LPD and LPD compared to NPD, at E12.5, E14.5 and E17.5 (fig 5D and See SI Appendix, fig. S4A). These results were confirmed by analyzing the proliferation of plated cells from E14.5 ganglionic eminences using Ki67 and BrdU as markers of proliferating cells and cells in S phase respectively. Growth fraction and mitotic index were calculated as the proportion of DAPI-labeled cells stained with Ki67 and with BrdU respectively, while the labeling index was calculated as the proportion of Ki67-labelled cells stained with BrdU. A significant decrease of all three proliferation indices was present in LPD compared to NPD and in the mitotic and labeling indices for Emb-LPD (See SI Appendix, fig. S4C-E). Thus maternal Emb-LPD and LPD reduce the proliferation of ganglionic eminences and cortex cells in the VZ where most NSCs are located, thereby potentially contributing to the loss of NSCs reported above.

Maternal protein restriction increases apoptosis of ganglionic eminences and cortex cells.

Cell death through apoptosis is another mechanism by which cell numbers might be regulated and we thus analyzed apoptosis by immunostaining for activated cleaved caspase-3 on coronal sections (fig 5F-H). Quantification of the number of positive cells per area revealed that apoptotic cell numbers significantly increased in LPD in all three layers of the ganglionic eminences (fig 5E) and cortex (See SI Appendix, fig. S4B) at E17.5. It was also significantly increased in Emb-LPD VZ and SVZ/IZ at E17.5 (fig 5E and See SI Appendix, fig. S4B). However, there was no difference in both Emb-LPD and LPD at both E12.5 and E14.5, compared to NPD. This increase in apoptosis at E17.5 in LPD may further explain why the increased proportion of late neuronal progenitors do not lead to a proportionate increase in neurons formed.

Maternal protein restriction induces adult offspring short-term memory defects and

permanently alters neuronal ratio in adult cortex.

To see if the alterations at fetal stages persist into adulthood and cause behavioral phenotype, adult offspring were subject to behavioral tests. Novel object recognition tests were performed at 41 (fig 6A), 64 (fig 6B) and 96 (fig 6C) days after birth to test short-term memory. Our results show that the Emb-LPD group performed significantly worse at all three time points, compared to the NPD group, with a discrimination index between novel and familiar object close to 0, showing no greater time spent to explore the novel object. The LPD group showed no difference with the NPD group. There was no difference in anxiety shown by the elevated-plus maze tests among the groups for both gender. At time of death, weights were taken and offspring male and female body weights and brain/body ratio were significantly different for Emb-LPD compared to NPD groups (table 2), with no significance for LPD compared to NPD. In order to see if the fetal brain cytoarchitecture changes persisted in the adult and correlated with the behavior phenotype, cortex of the adult offspring were analyzed for cortex thickness, neuron ratio and gene expression. Our data show that somatosensory cortex thickness is significantly increased in the Emb-LPD group compared to both NPD and LPD groups (fig 6D). To explore neuronal density, cortex was stained for NeuN, a mature neuron marker (fig 6 E-G), and positive cells were counted, compared to total cell numbers. Our data show that the neuronal density NeuN+/DAPI+ is significantly increased in layer IV, in Emb-LPD compared to NPD mice (fig 6H). The LPD group show significant neuronal density decrease in layer VI compared to the NPD group. Our data show that the increased neuronal ratio observed at fetal stage persists in the adult cortex and relates to the short-term memory defects in the Emb-LPD group, compared to both NPD and LPD groups.

Maternal protein restriction decreases fragile X gene family RNA levels in adult cortex.

Following some RNA sequencing analysis of related samples from our model, some candidate genes were selected to be tested in cortex samples. To explore possible molecular mechanisms responsible for the cellular and behavior changes, we performed qRT-PCR for genes known to be involved in cognitive functions such as short-term memory and shortlisted in our RNA sequencing analysis. Our data show that the RNA levels of *fragile X mental*

retardation 1 (*Fmr1)*, *fragile X mental retardation autosomal homolog* (*Fxr) 1 and 2,* and *Tyrosyl-DNA-phosphodiesterase 2 (Tdp2)* are decreased in the LPD adult cortex compared to NPD group, with *Fxr1, Fxr2* and *Tdp2* also decreased in the Emb-LPD group (fig 6I). This relates to the behavior and cellular phenotype observed in the Emb-LPD animals, with an independent cellular compensatory mechanism taking place in the LPD group.

Discussion

We have shown, using *in vivo* and *in vitro* techniques, that Emb-LPD and sustained LPD reduce NSCs/progenitor cell numbers through suppressed proliferation rates in both ganglionic eminences and cortex of the fetal brain at three different time points. Moreover, we find that the diminished stem cell pool after dietary treatment exhibits distinct differentiation dynamics with Emb-LPD inducing an increase in late neuronal progenitors and young neurons while LPD induced an increase in late neuronal progenitors but not in young neurons. Our study therefore shows that maternal protein restriction even during a very short and early period (Emb-LPD), leads to later effects on NSCs/progenitor cells, possibly due to a decrease in proliferation and an increase in apoptosis. However, for clarity, the timing of these effects during fetal development may not necessarily occur during preimplantation development but may derive subsequently up to the time of our fetal analyses.

Our data further indicate that compensatory processes are put in place to alleviate the effects of the stem cell deficit but vary according to diet treatment. Thus, whilst both LPD and Emb-LPD respond by increased progenitor neuronal differentiation, only in LPD is this potential excess of neurons tempered, possibly by the increased apoptosis observed, while in Emb-LPD an overproduction of neurons occurs in a growth-promoting environment of nutrient availability (discussed below). This leads to an increased cortical neuron ratio in adulthood and associates with short-term memory defect and decreased RNA levels of fragile X gene family in adult cortex. Collectively, our results add insight to the growing literature on the impact of maternal undernutrition on the offspring brain: while later gestation and perinatal challenge induces defects in brain neurochemistry (9), including decreased dopamine or increased serotonin levels (11-13), together with behavioral and cognitive defects (8), our data show that diet challenge from conception can cause comprehensive change in brain

structural development and neurogenesis with enduring effects on behavior and memory.

How might the altered patterns of brain development reported here, and with distinct outcomes between Emb-LPD and LPD treatments, derive? Previously, we have shown the early embryo before implantation may sense maternal Emb-LPD through deficient nutrient availability within uterine luminal fluid leading to suppression of blastocyst mTORC1 signaling (15), a dietary-induced mechanism that may also function in the human (16). Blastocyst sensing of poor maternal nutrients activates compensatory responses within extra-embryonic lineages which collectively lead to the development of a more efficient placenta and yolk sac (6, 7, 17, 18). However, in contrast, early undifferentiated embryonic lineages, studied using embryonic stem cell lines derived from Emb-LPD and NPD blastocysts, exhibit reduced cellular survival including reduced ERK-1/2 signaling and increased apoptosis (19), a phenotype consistent with the reduced NSCs pool found in the Emb-LPD and LPD fetal brain and associated increase in detection of cellular apoptosis. A further characteristic of later embryonic lineages in fetal somatic tissues such as liver and kidney relates to differential growth rate with continued LPD challenge suppressing ribosome biogenesis whilst release from this challenge (as in Emb-LPD) stimulating ribosome biogenesis relative to NPD controls, thereby coordinating growth with nutrient availability (20).

Thus, within the context of the current study on brain development, we interpret the initial reduction in NSCs found in both Emb-LPD and LPD samples as a consequence of either adverse dietary programming of undifferentiated cells, although the mechanism of induction is currently unknown, or maternal carry over effects. Subsequently, during fetal development, whilst both the Emb-LPD and LPD fetuses will be responsive to compensatory extra-embryonic systems, only the Emb-LPD fetuses will be in a ‘catch-up’ growth environment. Indeed, Emb-LPD offspring have increased mass during late gestation and postnatally compared with LPD and NPD offspring(6). Given these distinct characteristics, the Emb-LPD brain phenotype of reduced NSCs but leading to stimulated neurogenesis across the E12.5 to E17.5 time course and increased neuron ratio in the adult, compared to NPD, may reflect these systemic changes in programming environments. In contrast, the LPD brain, following

NSCs loss, will be within a more restrained growth environment, limiting the rate of neurogenesis.

Although these systemic factors may induce and contribute to the distinct embryonic programming mediated through maternal Emb-LPD and LPD, we need to further consider more specific factors that may influence fetal brain development. One candidate linking maternal LPD with offspring brain phenotype is docosahexaenoic acid (DHA). DHA concentration has been shown to be reduced in maternal liver and plasma after maternal LPD leading to a specific impaired accumulation of DHA in the offspring fetal brain (21, 22). DHA has been shown to increase neurosphere formation (23), which is consistent with the decrease in neurosphere formation shown here with LPD and Emb-LPD. DHA has also been shown to increase neuronal differentiation (beta-III-tubulin and MAP-2 positive cells) by decreasing Hes1 and increasing p27, thus leading to a cell cycle arrest of the NSCs (24). Hes1 itself is important for NSCs maintenance (25, 26). This was confirmed by others showing increase in beta-III-tubulin and MAP2 via activation of the PKA and CREB pathway (27). This might explain the effect of LPD on NSCs, but what about the Emb-LPD? Here, in the Emb-LPD group, the LPD stops at E3.5, a few days before the NSCs population is formed. However, the half-life of DHA in the rat brain (several weeks) (28) suggests that this specific effect of diet treatment may be long lasting and potentially retained in Emb-LPD up to the time of *in vivo* analysis.

Apart from its effect on NSCs, we show here that both maternal LPD and Emb-LPD have an effect on neuronal differentiation. Indeed, both treatments decrease the proportion of early progenitors while increasing the proportion of late progenitors. These results could be explained by specific alteration to the expression of the markers Nestin and beta-III-tubulin. Indeed, either higher expression of beta-III-tubulin in early progenitors or higher expression of Nestin in late progenitors would have led to higher proportion of late progenitors and lower proportion of neurons respectively. Such altered expression of Nestin has for example been observed in ischemic tissue damage (29), or following maternal restricted diet in the postnatal hippocampus (14). Alternatively, maternal LPD during fetal development (as opposed to Emb-

LPD) induces inhibition of differentiation of late progenitors into neurons. This disconnection between progenitor and neuron numbers has been described before in other contexts, where an increase in progenitor cells is not fully translated into the generation of mature neurons following a calorie-restricted diet (30) or in hippocampal adult neurogenesis (31). In our model, the mechanism ensuring the elimination of excess neurons is conserved in LPD, whereas it is disturbed in Emb-LPD, leading to increased neurons in late gestation compared with controls. Our data suggest that an early event in embryo development still affects neurogenesis in later pregnancy (discussed above) and neuron ratio in adulthood. E14.5 is the time in cortex development where 70% of the cells generated undergo programmed cell death (32) and our data suggest LPD and Emb-LPD could affect this process in distinct ways, as also identified in undifferentiated embryonic stem cell lines (19).

We identified a decrease in the Fragile X family genes RNA levels in Emb-LPD and LPD, which coincide with our behavioral deficit and altered cellular phenotype in Emb-LPD, with an independent compensatory mechanism taking place in the LPD group, to restore normal neuron proportion and behavior. FRM1P, FXR1P and FXR2P are neuronal RNA-binding proteins, involved in fragile X syndrome. They have the ability to interact and compensate each other as *Fmr1* and *Fxr2* double-knockout mice display more severe neurobehavioral abnormalities compared to single-knockout mice (33). *Fmr1* or *Fxr2* knockout mice have memory and cognition defects (34-36), similar to our maternal protein restriction model. FRM1P is also associated with Topoisomerase 3β (37, 38), which is itself a plausible substrate of TDP2 (39, 40) and is associated with cognitive impairment (37, 41). We thus speculate that the decrease in Fragile X family genes RNA levels highlights a molecular mechanism that could be responsible for our behavioral and cellular phenotype.

In conclusion, we find that maternal protein restricted diet, even exclusively before embryo implantation, can alter the developmental program and lead to permanent deficits in the offspring brain, reducing NSCs, altering the dynamics of neuronal differentiation and associating with behavioral defects. As discussed, our data strengthens the existing literature on early embryo sensing of dietary quality, with understanding on the adverse consequences on fetal brain development and adult offspring changes in behavior.

Materials and Methods

Animals: All mice and experimental procedures were conducted using protocols approved by, and in accordance with, the UK Home Office Animal (Scientific Procedures) Act 1986 and local ethics committee at the University of Southampton under UK Home Office Project License PPL30/2467 and PPL30/3001. Animals were housed in a SPF facility with 12 hours day-night cycles. Prior to treatment the animals were housed typically 5 per cage in conventional caging with aspen sawdust and sizzle nest enriched with plastic tubing and domes. All mice had food and water *ad libitum* and were fed a maintenance RM1 diet (Special Diet Services, Ltd., Witham, Essex, U.K) before treatments and where relevant, postnatally with pups weaned at 21 days. Maternal dietary treatments were conducted as previously described (6). Briefly, virgin female MF-1 outbred mice (aged 7–8.5 weeks) were randomly allocated to one of three isocaloric dietary treatment groups, being fed *ad libitum* with free access to water, either low protein diet (LPD; 9% casein) or normal protein diet (NPD; 18% casein) (18), throughout gestation only (termed LPD and NPD respectively) or exclusively during preimplantation development (from vaginal plug identification until 3.5 days; termed Emb-LPD) before being switched to NPD for the remainder of gestation. On the morning of the experiments, dams were sacrificed by cervical dislocation at E12.5, E14.5 or E17.5 in the laboratory, and fetuses decapitated for brain dissection or processed for subsequent experimentation. For adult offspring analysis, 3 cohorts of 3-4 litters were staggered across several months, with a total of 3-4 litters per group. In each cohorts, each group was represented by 1 or 2 litters. The same diet regime was followed as the fetal experiments, followed by RM1 during lactation and to offspring after weaning at 21 days. Litters were normalized to four males and four females at birth. In the morning of the 109th or 110th day after birth, mice were transcardially perfused with 0.9% NaCl containing 5 units/ml heparin sodium (CP Pharmaceuticals, UK), brains were cut in half sagittally, with one half fixed in 4% paraformaldehyde (PFA) and the other half dissected further into cortex, hippocampus, subventricular zone, cerebellum and striatum samples and snap frozen in liquid nitrogen. For all experiments, numbers of mothers and fetuses/offspring per treatment and experimental replicates used are recoded in figure legends.

Behavior, Novel object recognition assay: At 41, 64 and 96 days old, each animal was

subjected to the novel-object recognition test. Two objects (can 7 cm high, 3 cm diameter; square sand jar 7 cm high, 3.5 cm width, heavy enough not to be moved by the mice) were placed at equal distance from the top left corner and the bottom right corner respectively of the open arena (no bedding, 28.5 × 28.5 × 25 cm^3). The object combinations were changed randomly throughout all trials. All trials were video recorded (camera above the arena). Tests involved two phases, the acquisition and retention trials, with 1 minute between. During acquisition, individual animals were placed into the arena facing the top right corner with two identical objects for 4 minutes, before being removed and placed back into the home cage for one minute while the arena was cleaned with a 70% ethanol solution. The animals were replaced in the arena for the retention trial, with one of the two familiar objects randomly replaced with a novel item for a further 4 minutes. Video footage from the retention trial was used for analysis data, in random and blinded order, of exploration behaviour (normalized score for smell or nose touch of the object) and duration. Exploration time for the novel object (Tn) and the familiar object (Tf) during the retention trial were used to calculate the discrimination index DI = (Tn-Tf) / (Tn+Tf).

Neurosphere Culture: On harvesting, all tissues were mechanically dissociated to single cell suspensions according to established protocols for culture of fetal NSCs (42, 43), and cultured in single cell suspension at a density of 10 cells/μL. Growth medium consisted of Neurobasal-A (Invitrogen), supplemented with B27, L-glutamine 2 mM, antibiotic/antimycotic preparation, and growth factors (human FGFb 10 ng/mL, human EGF 20 ng/mL and heparin 2 μg/mL). Sphere counts were performed at day 7 and reflect the number of spheres >100 μm in diameter per well, averaged across at least 3 wells per sample. Spheres were passaged after 8 days. Passaging was accomplished by centrifugation, then 25 cycles of mechanical trituration using a 1 mL pipette, followed by resuspension at 10 cells/μL in fresh medium.

In Vitro Proliferation Analysis: Monolayer cultures were used to assess proliferation 3 days after cell plating. Cells in these cultures were plated at equal live cell density on coverslips coated with 0.01% poly-L-ornithine and 50 μg/mL laminin. BrdU labeling was used to allow determination of mitotic and labeling indices by exposing the cultures to 20 μM BrdU over a period of 5 hours, followed by fixation and immunostaining. Growth fraction and mitotic index

were calculated as the proportion of DAPI-labeled cells stained respectively with Ki67 and BrdU. Labeling index was calculated as the proportion of Ki67-labelled cells stained with BrdU.

Flow cytometry analysis of markers: Cells were incubated in reagents from the fixable Live/Dead Violet Viability stain (Invitrogen, Paisley, United Kingdom) before being treated with BD Cytofix/Cytoperm kit (554714). Cells were then incubated with Phycoerythin-anti-Nestin (IC2736P, R&D systems) and Alexa Fluor® 488 anti-Tubulin Beta 3 (Biolegend) or their matching isotype control antibodies. Phenotypic characterization of cells was performed with a 9-color FACSAria cell sorter and FACSDiva Software (version 5.0.3; BD Biosciences, Oxford, United Kingdom).

Immunostaining and Quantification: Tissue 14 μm sections were obtained by fixing brains in 4% PFA and sectioning on a cryostat. Cultured cells were fixed in 4% PFA. For BrdU staining, cells were incubated with 2 M hydrochloric acid before staining. Staining was performed on cells and sections using antibodies : mouse anti-Nestin (Millipore mab353, 1:100), mouse anti-Beta-III-tubulin (Covance mms-435p-250, 1:500), mouse anti-BrdU (Sigma B2531, 1:200), rabbit anti-Ki-67 (Vector Labs VP-RM04, 1:50), goat anti-Sox2 (Santa Cruz SC-17320, 1:50), rabbit anti-cleaved caspase-3 (Cell Signalling Technologies 9664, 1:400). Secondary antibodies used were Donkey Alexa Fluor 488 and 568 (Invitrogen 1:200) raised against appropriate primary sera. For NeuN staining on adult brain sections, post-fixation was performed with 4% PFA for 20 minutes followed by a heat shock citrate buffer (0.01M pH 6.0) antigen retrieval step. PBS with 0.2% TritonX-100 was used to permeabilise the tissue and 10% donkey serum in PBS for 1 hour at 37°C to block non-specific epitopes. The primary antibody mouse anti-NeuN (Millipore MAB377 clone A60 1:250) was added in PBS 10% donkey serum and left to incubate at 4°C overnight. The sections were permeabilised for 20 minutes again on the second day after which the secondary antibody (488 Alexa Fluor donkey anti-mouse (Thermoscientific A21202 1:200) was added in PBS 10% donkey serum and left to incubate at 37°C for 2 hours. DAPI incubation (Calbiochem CAS 28718-90-3 1 mg/mL) was carried out for 5 minutes before mounting the slides.For each marker, sections were stained and analyzed using Image J. The density of staining (pixel intensity within an area) was analyzed for Beta-III-tubulin, within at least three randomly

selected fields. For Ki67, cleaved caspase-3, Sox2 and NeuN, the number of positive cells were counted per field and compared to DAPI+ cell numbers within at least three randomly selected fields per layer per image. With at elast 3 images per brain.

Cortex thickness: Images of the somatosensory cortex were taken from DAPI stained sections and analyzed using ImageJ. One thickness measurement was taken per image, with 3 images per brain. Measures were taken in µm.

qRT-PCR: RNA was isolated using a lipid tissue RNA isolation kit and protocol from Qiagen, Inc. (Valencia, CA). Snap frozen brain cortex regions were homogenized using a handheld electric homogenizer with the QIAzol reagent. RNA was eluted from the midi columns with two aliquots of 250µL each of RNase-free water. Concentration and RNA integrity was measured by a bioanalyzer (Agilent, UK). RNA samples were stored at -80°C until use. 1ug RNA was transcribed into cDNA using the iScript cDNA synthesis kit (Biorad, UK) as per the manufacturer's protocol for a 20µl reaction using a PTC240 tetrad 2 peltier thermal cycler (MJ research, Canada). cDNA was stored at -20°C. qPCR was then performed using SYBR green (Primer design, UK) on a C1000 Thermal Cycler with a CFX96 detection module (Bio-Rad, UK). MJ Opticon Monitor Software (Bio-Rad, UK) was used to plot fluorescent intensity over time and C(t) values were calculated for each marker at the auto-calculated threshold. Melting curves in 0.2°C intervals between 55°C to 90°C were compiled to ensure that the template was amplified specifically. C(t) values for glyceraldehyde-3-phosphate dehydrogenase (*Gapdh*) and Adaptor Related Protein Complex 3 Delta 1 Subunit (*Ap3d1*) levels were measured for each cDNA sample as reference C(t) values. Reference genes were selected using the 12 geNorm kit (Primer design, UK). C(t) values were obtained and relative *gene* expression levels were calculated by normalizing the *gene* C(t) values to the *Gapdh* and *Ap3d1* C(t) values using the 2-ΔΔC(t) method such that relative expression = 2(C(t) *Gapdh&Ap3d1* – C(t) *gene*) . Primers for *Fxr1*, *Fmr1*, *Tdp2*, *Ap3d1* and *Gapdh* are proprietary property of PrimerDesign. Primers used for *Fxr2* were FXR2_forward: TCAGGACAGAAGGGTGACTC and FXR2_reverse: GAAAGGAGGGATGTGGACCG.

Statistical analysis: Unless otherwise stated, data were analyzed using a multilevel linear regression model using PASW for Windows program version 21 (SPSS UK, Woking, Surrey, United Kingdom)***,*** in which there was a random effect assigned to each litter. Thus we

evaluated both between-litter and within-litter effects. We always included terms for the litter size and for the sex of the offspring, where appropriate. We used indicator variables to compare the Emb-LPD and the LPD with the NPD. This showed that differences identified between treatment groups are independent of maternal origin of litter and litter size *(44)*. Boxes represent interquartile ranges with middle lines representing the medians, whiskers (error bars) above and below the box indicate the 90th and 10th percentiles. *p<0.05, **p<0.01, ***p<0.001, ****p<0.0001

Acknowledgments:

The studies reported here were supported through awards from Faculty of Medicine-University of Southampton, Wessex Medical Research and Rosetrees Trust (M327-CD1) to SWM, the Biotechnology and Biological Sciences Research Council (BB/I001840/1, BB/F007450/1), the EU-FP7 EpiHealth programs and the Gerald Kerkut Trust to TPF, The Leonard Thomas fund to LEA, Dr Sanderson bursary to LEA and PJS, the Wolfson Foundation to CJA. Funders had no role in the conception and design of the study, provision of study material, collection of data, data analysis and interpretation or manuscript writing. We thank Prof Clive Osmond for help with statistical analysis, staff from the University of Southampton Biomedical Research Facility for animal provision and maintenance and the Flow Cytometry Unit, Faculty of Medicine, University of Southampton for flow cytometry assistance and maintenance.

Disclosure of potential conflicts of interests:

None

References

1. Barker DJ, Osmond C, Kajantie E, & Eriksson JG (2009) Growth and chronic disease: findings in the Helsinki Birth Cohort. *Annals of human biology* 36(5):445-458.
2. Barker DJ & Thornburg KL (2013) The obstetric origins of health for a lifetime. *Clinical obstetrics and gynecology* 56(3):511-519.
3. Raikkonen K*, et al.* (2013) Early life origins cognitive decline: findings in elderly men in the Helsinki Birth Cohort Study. *PLoS One* 8(1):e54707.
4. Wahlbeck K, Forsen T, Osmond C, Barker DJ, & Eriksson JG (2001) Association of schizophrenia with low maternal body mass index, small size at birth, and thinness during childhood. *Archives of general psychiatry* 58(1):48-52.
5. Roseboom TJ, Painter RC, van Abeelen AF, Veenendaal MV, & de Rooij SR (2011) Hungry in the womb: what are the consequences? Lessons from the Dutch famine. *Maturitas* 70(2):141-145.
6. Watkins AJ*, et al.* (2008) Adaptive responses by mouse early embryos to maternal diet protect fetal growth but predispose to adult onset disease. *Biology of reproduction* 78(2):299-306.
7. Fleming TP*, et al.* (2015) Do little embryos make big decisions? How maternal dietary protein restriction can permanently change an embryo. *Reprod Fertil Dev* 27:684-692.
8. Akitake Y*, et al.* (2015) Moderate maternal food restriction in mice impairs physical growth, behavior, and neurodevelopment of offspring. *Nutr Res* 35(1):76-87.
9. Alamy M & Bengelloun WA (2012) Malnutrition and brain development: an analysis of the effects of inadequate diet during different stages of life in rat. *Neuroscience and biobehavioral reviews* 36(6):1463-1480.
10. Belluscio LM, Berardino BG, Ferroni NM, Ceruti JM, & Canepa ET (2014) Early protein malnutrition negatively impacts physical growth and neurological reflexes and evokes anxiety and depressive-like behaviors. *Physiol Behav* 129:237-254.

11. Kehoe P, Mallinson K, Bronzino J, & McCormick CM (2001) Effects of prenatal protein malnutrition and neonatal stress on CNS responsiveness. *Brain Res Dev Brain Res* 132(1):23-31.
12. Mokler DJ, Torres OI, Galler JR, & Morgane PJ (2007) Stress-induced changes in extracellular dopamine and serotonin in the medial prefrontal cortex and dorsal hippocampus of prenatally malnourished rats. *Brain Res* 1148:226-233.
13. Resnick O & Morgane PJ (1984) Ontogeny of the levels of serotonin in various parts of the brain in severely protein malnourished rats. *Brain Res* 303(1):163-170.
14. Amarger V*, et al.* (2014) Protein content and methyl donors in maternal diet interact to influence the proliferation rate and cell fate of neural stem cells in rat hippocampus. *Nutrients* 6(10):4200-4217.
15. Eckert JJ*, et al.* (2012) Metabolic Induction and Early Responses of Mouse Blastocyst Developmental Programming following Maternal Low Protein Diet Affecting Life-Long Health. *PLoS One* 7(12):e52791.
16. Kermack AJ*, et al.* (2015) Amino acid composition of human uterine fluid: association with age, lifestyle and gynaecological pathology. *Hum Reprod* 30(4):917-924.
17. Sun C*, et al.* (2014) Mouse early extra-embryonic lineages activate compensatory endocytosis in response to poor maternal nutrition. *Development* 141(5):1140-1150.
18. Watkins AJ, Lucas ES, Wilkins A, Cagampang FR, & Fleming TP (2011) Maternal periconceptional and gestational low protein diet affects mouse offspring growth, cardiovascular and adipose phenotype at 1 year of age. *PLoS One* 6(12):e28745.
19. Cox A, Fleming TP, & Smyth N (2011) Embryonic Stem Cells: Modelling Effects of Early Embryo Environment on Developmental Potential. *J Dev Orig Hlth Dis* 2:S93-S94.
20. Denisenko O*, et al.* (2016) Regulation of ribosomal RNA expression across the lifespan is fine-tuned by maternal diet before implantation. *Biochim Biophys Acta* 1859(7):906-913.
21. Burdge GC, Dunn RL, Wootton SA, & Jackson AA (2002) Effect of reduced dietary protein intake on hepatic and plasma essential fatty acid concentrations in the adult

female rat: effect of pregnancy and consequences for accumulation of arachidonic and docosahexaenoic acids in fetal liver and brain. *Br J Nutr* 88(4):379-387.

22. Torres N*, et al.* (2010) Protein restriction during pregnancy affects maternal liver lipid metabolism and fetal brain lipid composition in the rat. *Am J Physiol Endocrinol Metab* 298(2):E270-277.
23. Sakayori N*, et al.* (2011) Distinctive effects of arachidonic acid and docosahexaenoic acid on neural stem /progenitor cells. *Genes Cells* 16(7):778-790.
24. Katakura M*, et al.* (2009) Docosahexaenoic acid promotes neuronal differentiation by regulating basic helix-loop-helix transcription factors and cell cycle in neural stem cells. *Neuroscience* 160(3):651-660.
25. Kageyama R, Ohtsuka T, & Kobayashi T (2008) Roles of Hes genes in neural development. *Dev Growth Differ* 50 Suppl 1:S97-103.
26. Ohtsuka T, Sakamoto M, Guillemot F, & Kageyama R (2001) Roles of the basic helix-loop-helix genes Hes1 and Hes5 in expansion of neural stem cells of the developing brain. *J Biol Chem* 276(32):30467-30474.
27. Rashid MA, Katakura M, Kharebava G, Kevala K, & Kim HY (2013) N-Docosahexaenoylethanolamine is a potent neurogenic factor for neural stem cell differentiation. *J Neurochem* 125(6):869-884.
28. DeMar JC, Jr., Ma K, Bell JM, & Rapoport SI (2004) Half-lives of docosahexaenoic acid in rat brain phospholipids are prolonged by 15 weeks of nutritional deprivation of n-3 polyunsaturated fatty acids. *J Neurochem* 91(5):1125-1137.
29. Korzhevskii DE, Lentsman MV, Gilyarov AV, Kirik OV, & Vlasov TD (2008) Induction of nestin synthesis in rat brain cells by ischemic damage. *Neurosci Behav Physiol* 38(2):139-143.
30. Park JH*, et al.* (2013) Calorie restriction alleviates the age-related decrease in neural progenitor cell division in the aging brain. *Eur J Neurosci* 37(12):1987-1993.
31. Plumpe T*, et al.* (2006) Variability of doublecortin-associated dendrite maturation in adult hippocampal neurogenesis is independent of the regulation of precursor cell proliferation. *BMC Neurosci* 7:77.

32. Blaschke AJ, Staley K, & Chun J (1996) Widespread programmed cell death in proliferative and postmitotic regions of the fetal cerebral cortex. *Development* 122(4):1165-1174.

33. Spencer CM*, et al.* (2006) Exaggerated behavioral phenotypes in Fmr1/Fxr2 double knockout mice reveal a functional genetic interaction between Fragile X-related proteins. *Hum Mol Genet* 15(12):1984-1994.

34. Bontekoe CJ*, et al.* (2002) Knockout mouse model for Fxr2: a model for mental retardation. *Hum Mol Genet* 11(5):487-498.

35. Nolan SO*, et al.* (2017) Deletion of Fmr1 results in sex-specific changes in behavior. *Brain Behav* 7(10):e00800.

36. Gaudissard J*, et al.* (2017) Behavioral abnormalities in the Fmr1-KO2 mouse model of fragile X syndrome: The relevance of early life phases. *Autism Res* 10(10):1584-1596.

37. Stoll G*, et al.* (2013) Deletion of TOP3beta, a component of FMRP-containing mRNPs, contributes to neurodevelopmental disorders. *Nat Neurosci* 16(9):1228-1237.

38. Xu D*, et al.* (2013) Top3beta is an RNA topoisomerase that works with fragile X syndrome protein to promote synapse formation. *Nat Neurosci* 16(9):1238-1247.

39. Gao R, Huang SY, Marchand C, & Pommier Y (2012) Biochemical characterization of human tyrosyl-DNA phosphodiesterase 2 (TDP2/TTRAP): a Mg(2+)/Mn(2+)-dependent phosphodiesterase specific for the repair of topoisomerase cleavage complexes. *J Biol Chem* 287(36):30842-30852.

40. Pommier Y*, et al.* (2014) Tyrosyl-DNA-phosphodiesterases (TDP1 and TDP2). *DNA Repair (Amst)* 19:114-129.

41. Gomez-Herreros F*, et al.* (2014) TDP2 protects transcription from abortive topoisomerase activity and is required for normal neural function. *Nat Genet* 46(5):516-521.

42. Reynolds BA & Weiss S (1992) Generation of neurons and astrocytes from isolated cells of the adult mammalian central nervous system. *Science* 255(5052):1707-1710.

43. Morshead CM*, et al.* (1994) Neural stem cells in the adult mammalian forebrain: a relatively quiescent subpopulation of subependymal cells. *Neuron* 13(5):1071-1082.
44. Watkins AJ*, et al.* (2007) Mouse embryo culture induces changes in postnatal phenotype including raised systolic blood pressure. *Proc Natl Acad Sci U S A* 104(13):5449-5454.

Figure legends

Figure 1: Maternal diet affects primary sphere formation from neural cells

(A) Experimental model describing the three diet groups with NPD group exposed to 18% protein diet throughout gestation, LPD group exposed to 9% protein diet from vaginal plug on E0.5 and Emb-LPD group exposed to 9% protein diet between E0.5 and E3.5 followed by 18% protein diet until time of analysis at E12.5, E14.5 or E17.5. For adult offspring, dams were switched to RM1 chow at birth and offspring were given RM1 from weaning. Key events of cortex and ganglionic eminences development relevant to our study are highlighted, with NSC proliferation spanning the fetal time points of the present analysis, neurogenesis peaking between E12.5 and E14.5 and young neurons apoptosis peaking at E14.5.

(B) Representative images of spheres generated from neural cells. Scale bar = 50µm. Quantification of the number of primary spheres (over 100µm in diameter) per well after 7 days with 5000 cells plated from the ganglionic eminences (C-E-G) or cortex (D-F-H) from the three maternal diet groups.

E12.5 ganglionic eminences and cortex data represent n=24 (NPD), 18 (Emb-LPD), 21 (LPD) fetuses from 8 (NPD), 6 (Emb-LPD) or 7 (LPD) mothers.

E14.5 ganglionic eminences data represent n=131 (NPD), 125 (Emb-LPD), 124 (LPD) fetuses from 17 (NPD), 17 (Emb-LPD) or 18 (LPD) mothers.

E14.5 cortex data represent n=18 (NPD), 18 (Emb-LPD), 19 (LPD) fetuses from 6 (NPD), 6 (Emb-LPD) or 6 (LPD) mothers.

E17.5 ganglionic eminences data represent n=18 (NPD), 18 (Emb-LPD), 21 (LPD) fetuses from 6 (NPD), 6 (Emb-LPD) or 7 (LPD) mothers.

E17.5 cortex data represent n=18 (NPD), 18 (Emb-LPD), 24 (LPD) fetuses from 6 (NPD), 6

(Emb-LPD) or 8 (LPD) mothers.

Boxes represent interquartile ranges with middle lines representing the medians, whiskers (error bars) above and below the box indicate the 90th and 10th percentiles. *p<0.05, **p<0.01, ***p<0.001, ****p<0.0001

Figure 2: Maternal diet affects expression of neural stem cells and neuronal differentiation markers analyzed by flow cytometry in ganglionic eminences cells.

Example of FACS plots with isotype control antibodies (A) and antibodies against Nestin and BetaIIItubulin (B), showing how ganglionic eminences cells were defined and gated: Nestin only positive cells (Q1), double positive cells (Q2) and BetaIIItubulin only positive cells (Q4). Double positive cells (Q2) were further separated into Nestin+ BetaIIItubulin dim (Q2N), and Nestin dim BetaIIItubulin+ (Q2B). A total of 10,000 cells were analyzed per sample.

Quantification by flow cytometry of E12.5 (C-F) E14.5 (G-J) and E17.5 (K-N) ganglionic eminences cells stained for Nestin and BetaIIItubulin.

Nestin only positive cells (C,G,K), double positive cells separated into Nestin+ BetaIIItubulin dim (D,H,L), and Nestin dim BetaIIItubulin+ (E,I,M), and BetaIIItubulin only positive cells (F,J,N) were quantified.

E12.5 ganglionic eminences data represent n=24 (NPD), 18 (Emb-LPD), 21 (LPD) fetuses from 8 (NPD), 6 (Emb-LPD) or 7 (LPD) mothers.

E14.5 ganglionic eminences data represent n=131 (NPD), 125 (Emb-LPD), 124 (LPD) fetuses from 17 (NPD), 17 (Emb-LPD) or 18 (LPD) mothers.

E17.5 ganglionic eminences data represent n=18 (NPD), 18 (Emb-LPD), 18 (LPD) fetuses from 6 (NPD), 6 (Emb-LPD) or 6 (LPD) mothers.

Boxes represent interquartile ranges with middle lines representing the medians, whiskers (error bars) above and below the box indicate the 90th and 10th percentiles. *p<0.05, **p<0.01, ***p<0.001, ****p<0.0001

Figure 3: Summary of flow cytometry data for ganglionic eminences primary cells.

(A) Summary of the FACS data at E12.5, E14.5 and E17.5 for ganglionic eminences primary cells from figure 2 C-N, with enlargement of the neural stem/progenitor cells data (Nestin+,

light blue, B). Early neuronal progenitors (Nestin+ Beta-III-tubulin dim, royal blue), late neuronal progenitors (Nestin dim Beta-III-tubulin+, purple) and neurons (Beta-III-tubulin+, dark blue) are presented along the differentiation lineage (black arrow).

Figure 4: Maternal diet affects expression of neuronal differentiation markers analyzed by immunohistochemistry in E14.5 ganglionic eminences and cortex.

Representative images illustrate the staining results quantified: Beta-III-tubulin (green, A-C) are stained on E14.5 ganglionic eminences sections from maternal NPD (A), Emb-LPD (B) and LPD (C). Scale bar=150µm.

Quantification of Beta-III-tubulin staining (% of positive pixels/area) on E14.5 ganglionic eminence (D) and cortex (E) sections from different maternal diets. Data represent 3 quantifications/layer/section of 3 sections/brain from 9 fetal brains from 9 different mothers per diet. Boxes represent interquartile ranges with middle lines representing the medians, whiskers (error bars) above and below the box indicate the 90th and 10th percentiles.

*p<0.05, **p<0.01, ***p<0.001, ****p<0.0001

N=NPD ; E=Emb=LPD ; L=LPD ; VZ=Ventricular Zone ; SVZ=Subventricular Zone; MZ=Mantle Zone ; IZ=Intermediate Zone ; CP=Cortical Plate

Figure 5: Maternal diet affects proliferation and apoptosis in ganglionic eminences.

(A-C) Representative images illustrate the staining results quantified in D: Ki67 (green), DAPI (blue) are stained on E12.5 ganglionic eminences sections from maternal NPD (A), Emb-LPD (B) and LPD (C).

(D) The growth fraction quantifies the proportion of cells (DAPI+) which are proliferating (Ki67+) in E12.5, E14.5 and E17.5 ganglionic eminences ventricular zone sections. Data represent 3 quantifications/layer/brain of 3 sections/brain of 5 fetal brains from 5 different mothers per diet.

(E) Quantification of Cleaved Caspase-3 staining (number of positive cells/area) on E17.5 ganglionic eminences sections. Data represent 3 quantifications/layer/brain of 3 sections/brain of 5 fetal brains from 5 different mothers per diet.

(F-H) Representative images illustrate the staining results quantified in (E): Cleaved

Caspase-3 (red) and DAPI (blue) staining of E17.5 ganglionic eminences subventricular zone sections from maternal NPD (F), Emb-LPD (G) and LPD (H).

Boxes represent interquartile ranges with middle lines representing the medians, whiskers (error bars) above and below the box indicate the 90th and 10th percentiles. *p<0.05, **p<0.01, ***p<0.001, ****p<0.0001

N=NPD; E=Emb=LPD; L=LPD; VZ=Ventricular Zone; SVZ=Subventricular Zone; MZ=Mantle Zone; Scale bar=50µm.

Figure 6: Maternal diet affects adult offspring short-term memory, cortical neuron ratio and Fragile X genes RNA levels.

(A-C) Discrimination index of familiar versus novel objects during the novel object recognition test at 41 days (A), 64 days (B) and 96 days (C). Data for exploration time for the novel object (Tn) versus the familiar object (Tf) are presented as the discrimination index DI = (Tn-Tf) / (Tn+Tf). Data collected from 14-22 animals from 3-4 mothers per group.

(D) Quantification of somatosensory cortex thickness in micrometers on adult brain sections in cortical layers I to VI. Data represent 1 quantification/brain of 3 sections/brain of 10 brains from 5 different mothers per diet.

(E-G) Representative images illustrate the staining results quantified in H: NeuN (green), DAPI (blue) are stained on adult female somatosensory cortical sections spanning layers I to VI, from maternal NPD (E), Emb-LPD (F) and LPD (G). Scale bar=100µm.

(H) Quantification of neuron ratio (ratio of NeuN positive cells versus DAPI positive cells) on adult somatosensory cortex sections in layers II/III to VI. Data represent 3 quantifications/layer/brain of 3 sections/brain of 10 brains from 5 different mothers per group.

(I) Quantification of *Fmr1, Fxr1, Fxr2* and *Tdp2* RNA levels by qRT-PCR, normalized to housekeeping genes *Ap3d1* and *Gapdh*. Data represent 1 sample/brain of 12-19 brains from 3 or 4 different mothers per group.

Both male and female adult offspring were analyzed. Offspring sex effects were not found using our multilevel linear regression model, thus representation of our data includes both males and females in balanced ratio. Boxes represent interquartile ranges with middle lines representing the medians, whiskers (error bars) above and below the box indicate the 90th

and 10th percentiles. *p<0.05, **p<0.01, ***p<0.001, ****p<0.0001. N=NPD; E=Emb=LPD; L=LPD.

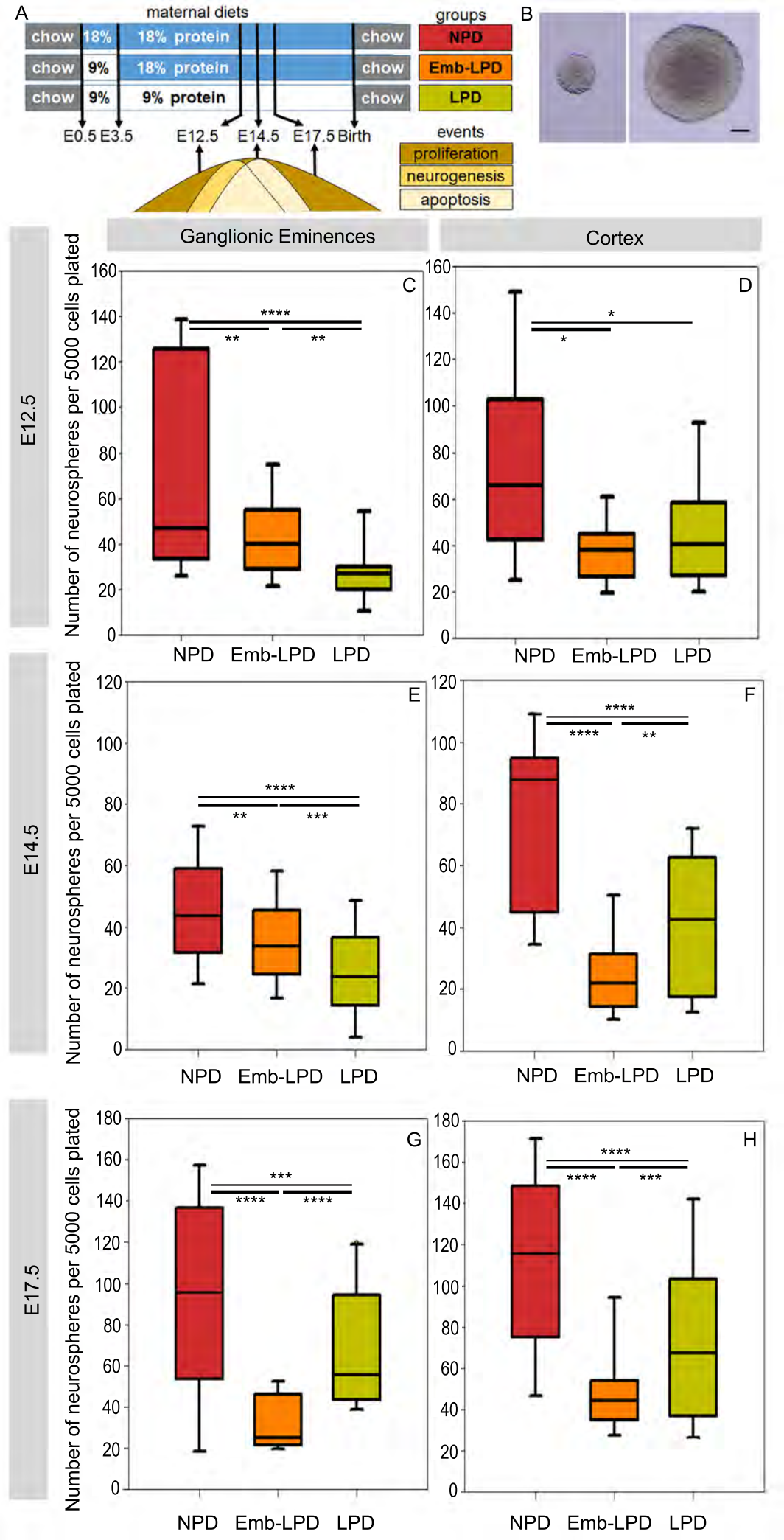
A
maternal diets
chow 18% 18% protein chow
chow 9% 18% protein chow
chow 9% 9% protein chow
groups
NPD
Emb-LPD
LPD
E0.5 E3.5 E12.5 E14.5 E17.5 Birth
events
proliferation
neurogenesis
apoptosis
B
Ganglionic Eminences
Cortex
E12.5
E14.5
E17.5
Number of neurospheres per 5000 cells plated
C
D
E
F
G
H
NPD Emb-LPD LPD

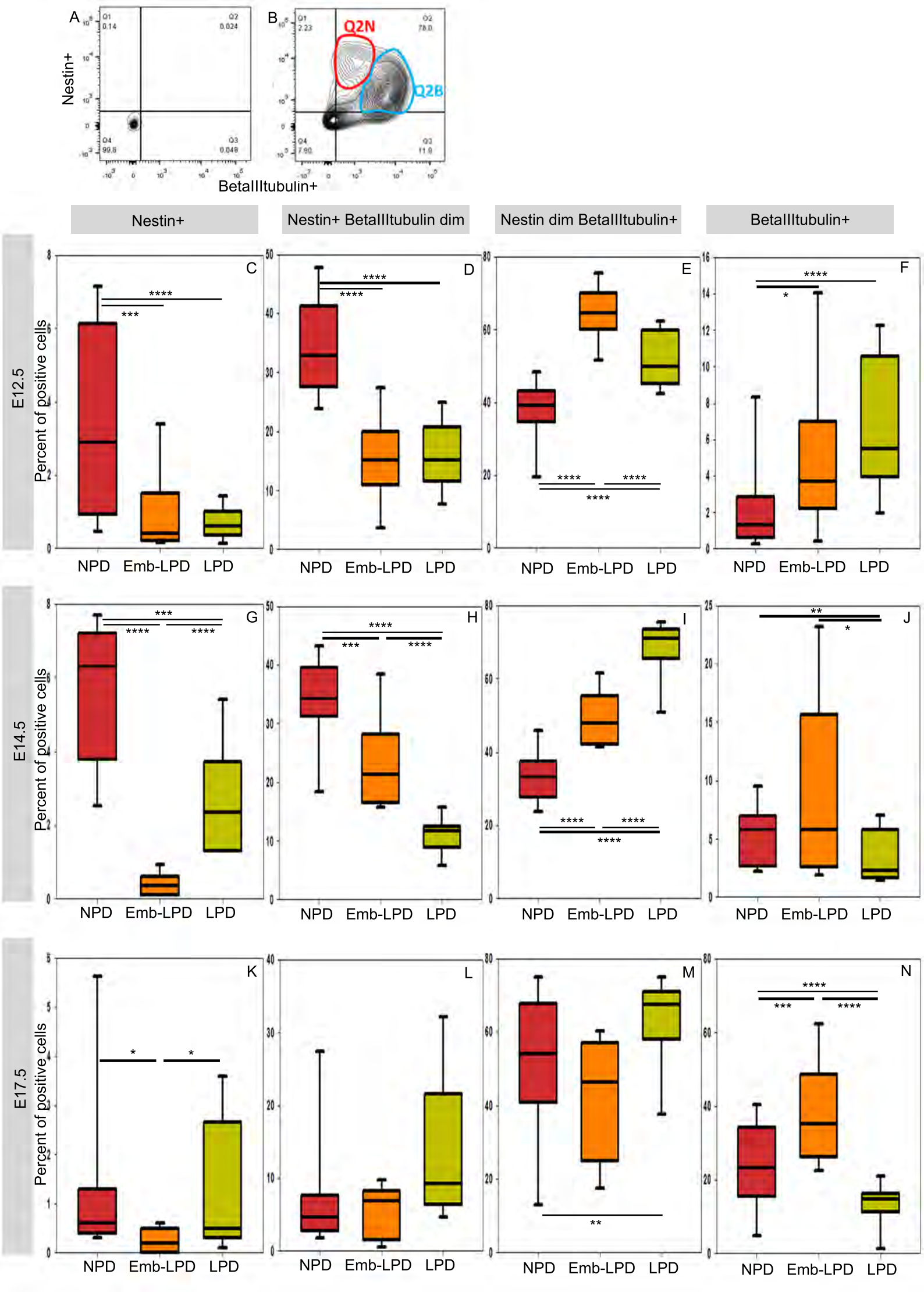
A
B
Q2N
Q2B
Nestin+
BetaIIItubulin+
Nestin+
Nestin+ BetaIIItubulin dim
Nestin dim BetaIIItubulin+
BetaIIItubulin+
E12.5
E14.5
E17.5
Percent of positive cells
NPD
Emb-LPD
LPD
C
D
E
F
G
H
I
J
K
L
M
N

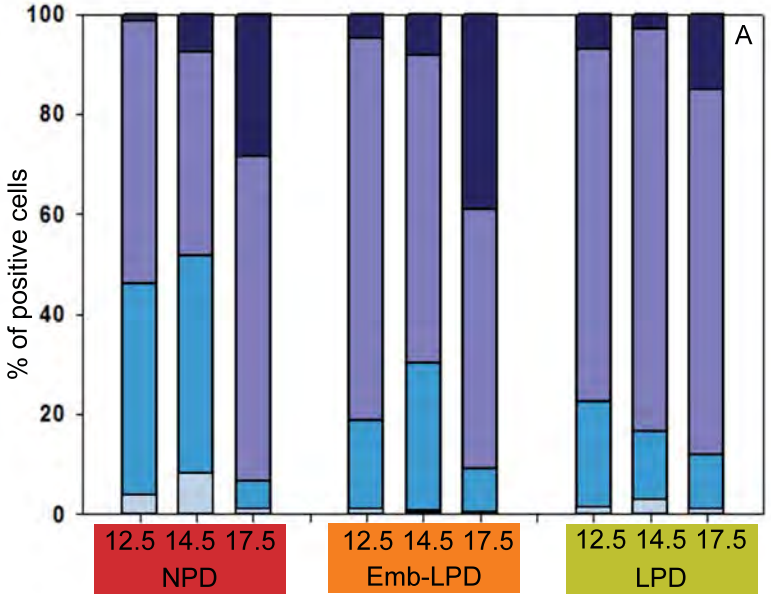
A
100
80
60
40
20
0
% of positive cells
12.5 14.5 17.5
NPD
12.5 14.5 17.5
Emb-LPD
12.5 14.5 17.5
LPD

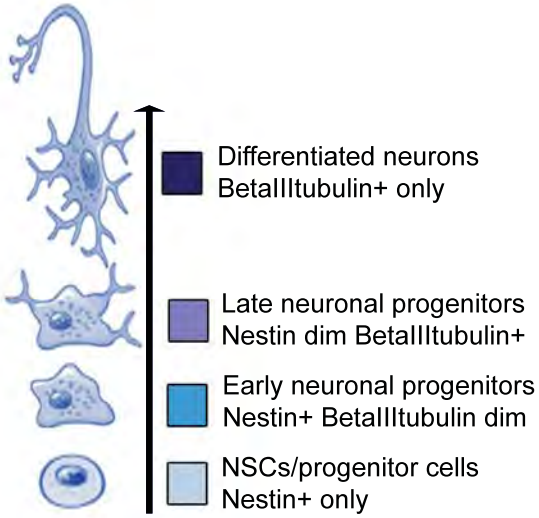
Differentiated neurons
BetaIIItubulin+ only
Late neuronal progenitors
Nestin dim BetaIIItubulin+
Early neuronal progenitors
Nestin+ BetaIIItubulin dim
NSCs/progenitor cells
Nestin+ only

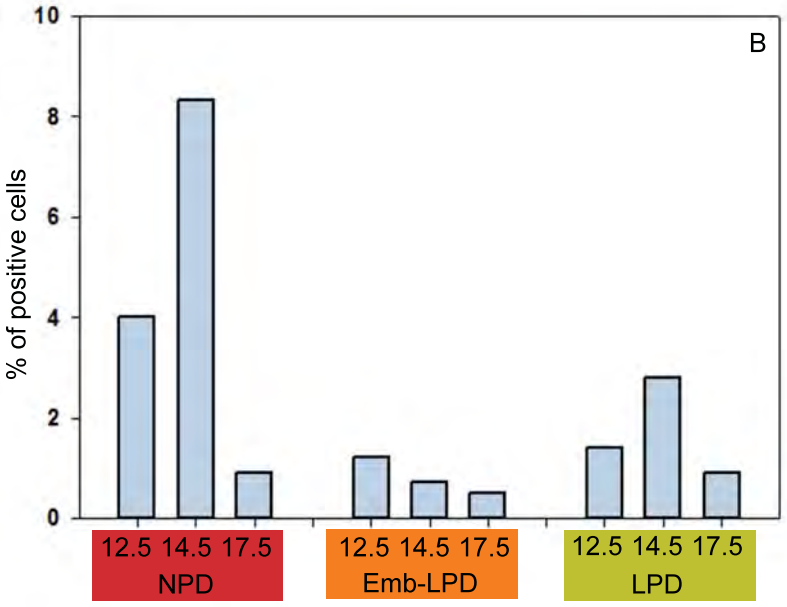
B
10
8
6
4
2
0
% of positive cells
12.5 14.5 17.5
NPD
12.5 14.5 17.5
Emb-LPD
12.5 14.5 17.5
LPD

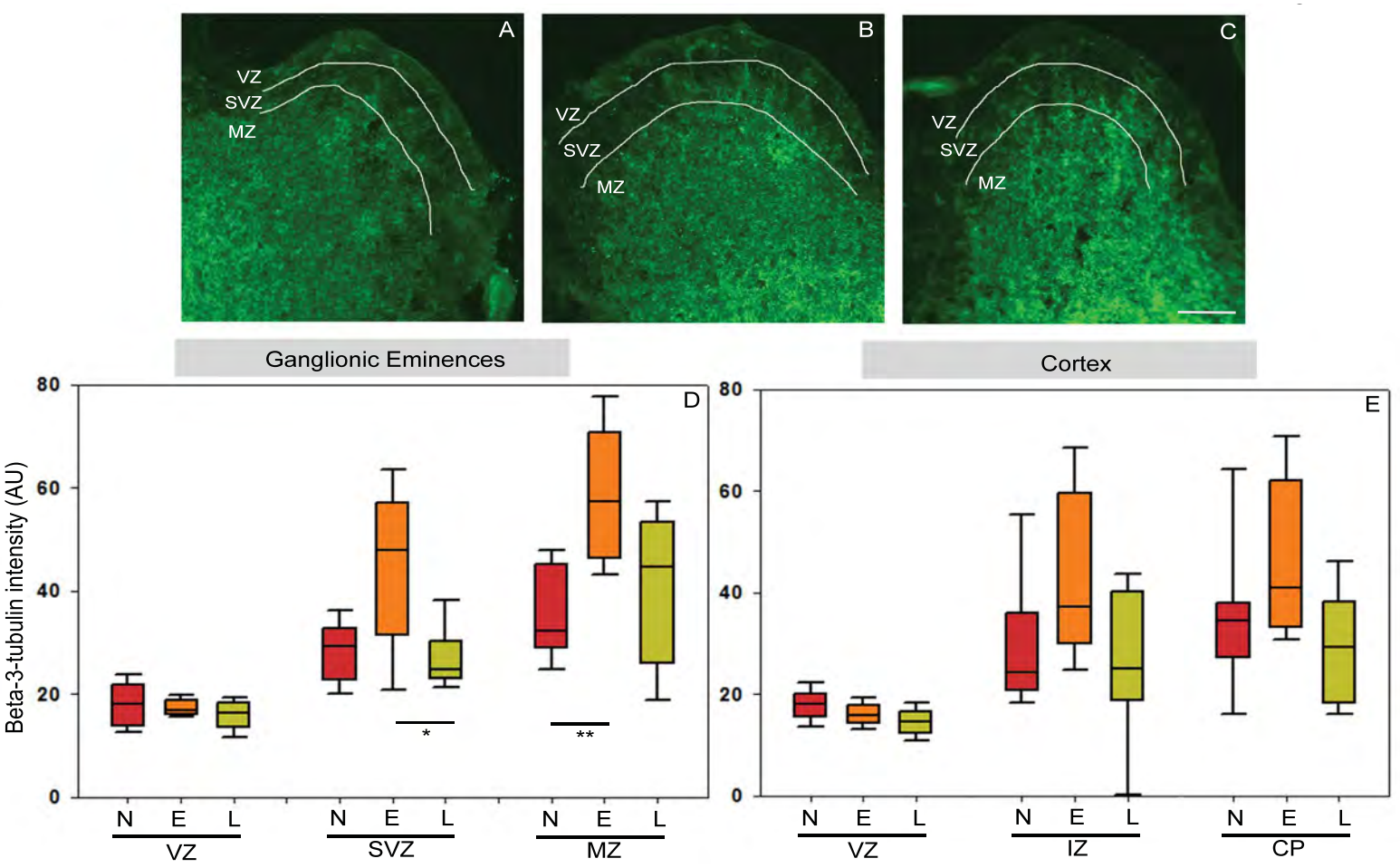
A
VZ
SVZ
MZ
B
VZ
SVZ
MZ
C
VZ
SVZ
MZ
Ganglionic Eminences
Cortex
D
E
Beta-3-tubulin intensity (AU)
0
20
40
60
80
N E L
VZ
SVZ
MZ
IZ
CP
*
**

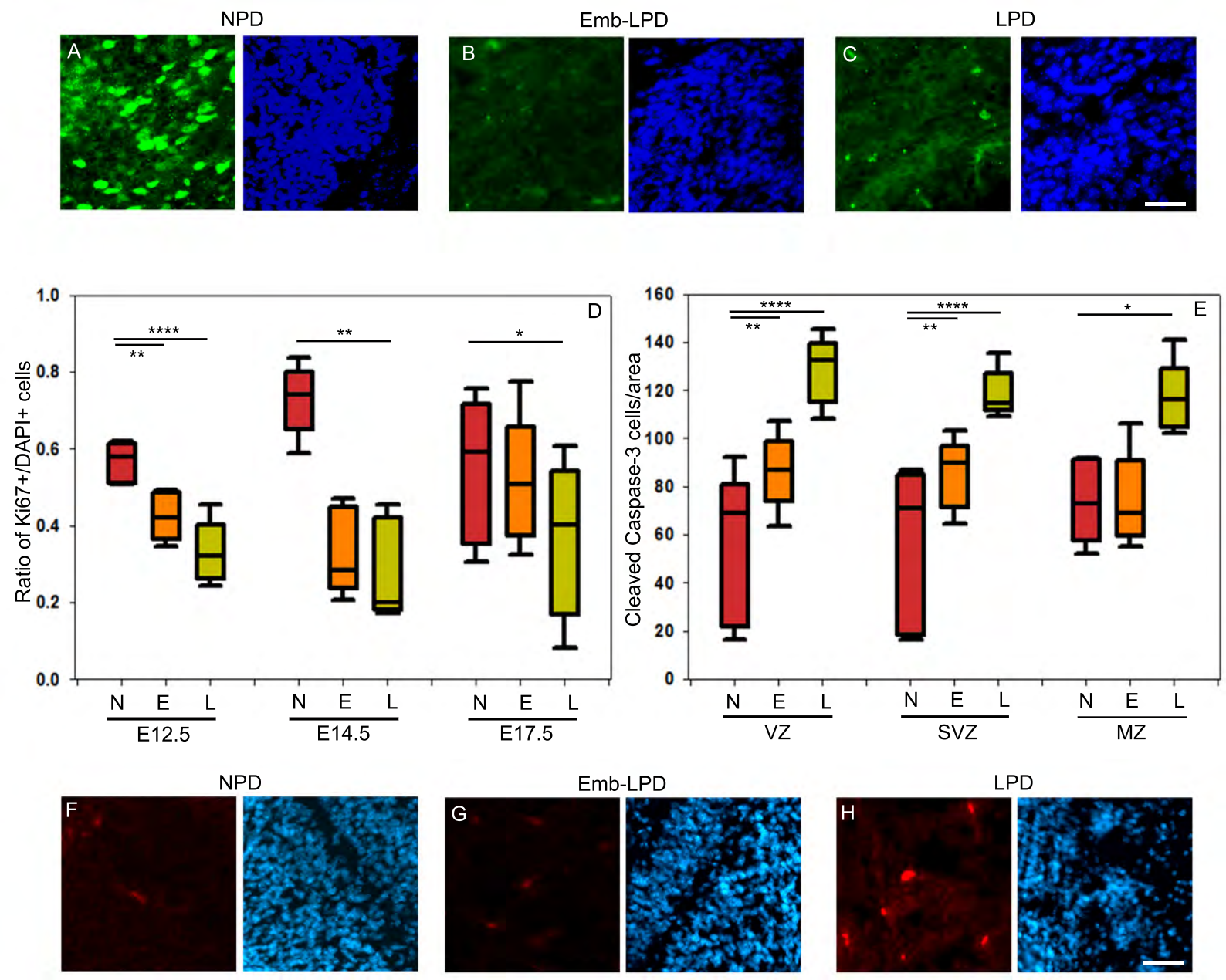
NPD
Emb-LPD
LPD
A
B
C
D
E
F
G
H
Ratio of Ki67+/DAPI+ cells
Cleaved Caspase-3 cells/area
N E L
E12.5
E14.5
E17.5
VZ
SVZ
MZ

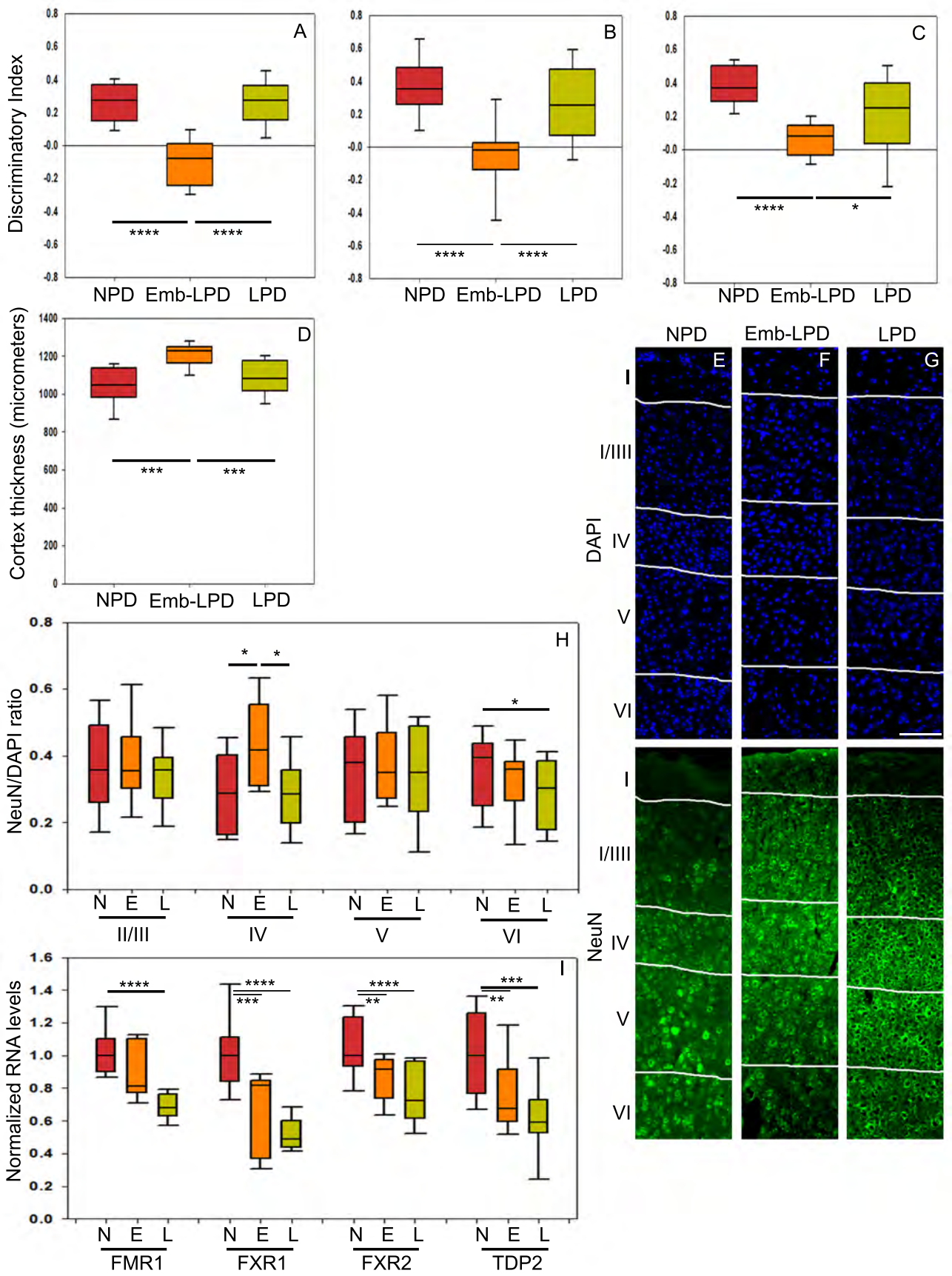
A
B
C
D
E
F
G
H
I
Discriminatory Index
Cortex thickness (micrometers)
NeuN/DAPI ratio
Normalized RNA levels
NPD
Emb-LPD
LPD
DAPI
NeuN
I
I/IIII
IV
V
VI
N E L
II/III
IV
V
VI
FMR1
FXR1
FXR2
TDP2

Table 1: Composition of normal and low protein diets. Normal protein diet (NPD, 18% protein) and low protein diet (LPD, 9% protein) are expressed as g/kg.

Component	NPD	LPD
Casein	180	90
Corn Starch	425	485
Sucrose	213	243
Corn oil	100	100
Fibre	50	50
AIN-76-mineral mix	20	20
AIN-76-vitamin mix	5	5
DL-methionine	5	5
Choline Chloride	2	2

Table 2: Weight of female and male offspring at time of death. Significant differences were found between the groups for body weight for Emb-LPD vs NPD (*p<0.05), and the brain/body ratio for Emb-LPD vs NPD (**p<0.01) and vs LPD in males (#p<0.05). Significant effect of sex was also found for body weight and brain /body ratio (+p<0.05; +++p<0.001 comparing males vs females), but not for brain weight (p>0.05). No significant intercation between treatment and sex were found. Boldface highlights values different between groups (* and #), which are the important differences within the context of our study. The sex effect (+) is not novel but is reported for sake of completeness. IQR, interquartile range.

		NPD		Emb-LPD		LPD	
		median	IQR	median	IQR	median	IQR
females	body weight (g)	37.75	36.82-39.22	**40.42 ***	36.89-42.57	37.03	34.80-39.36
	brain weight (g)	0.49	0.48-0.51	0.48	0.47-0.49	0.49	0.45-0.49
	brain/ body	0.0130	0.0125-0.0136	**0.0116 ***	0.0112-0.0131	0.0132	0.0115-0.0139
males	body weight (g)	43.37 +++	42.01-46.12	**45.34 * +++**	44.15-49.36	42.66 +++	41.05-46.32
	brain weight (g)	0.49	0.45-0.50	0.49	0.47-0.49	0.48	0.47-0.50
	brain/ body	0.0117 +	0.0107-0.0130	**0.0102 ** # +++**	0.0093-0.0109	0.0111 +	0.0106-0.0119

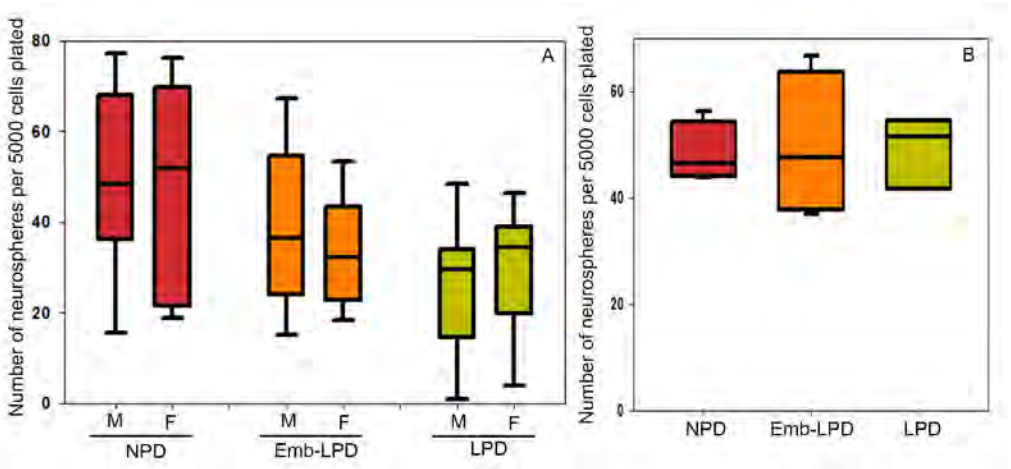

Fig S1: (A) Maternal diet effect on primary spheres is not affected by sex of the fetus. Quantification of the number of primary spheres per well after 7 days with 5000 cells plated from E14.5 ganglionic eminences from different maternal diets sorted by sex of the fetus. Data represent n=19 (NPD-M), 18 (NDP-F), 14 (Emb-LPD-M), 17 (Emb-LPD-F), 11 (LPD-M), 13 (LPD-F) fetuses from at least 7 mothers per group. Data analyzed by two way ANOVA showing a diet effect ($p<0.001$) but not sex effect ($p=0.866$) and no interaction between diet and sex ($p=0.769$).
(B) Maternal diet does not affect secondary sphere formation. Quantification of the number of secondary spheres per well after 7 days with 5000 cells plated from primary spheres from E14.5 ganglionic eminences from different maternal diets. Data represent n=4 (NPD), 4 (Emb-LPD), 3 (LPD) mothers with at least 6 wells from at least 2 fetuses.
Boxes represent interquartile ranges with middle lines representing the medians, whiskers (error bars) above and below the box indicate the 90th and 10th percentiles.
M=male; F=female

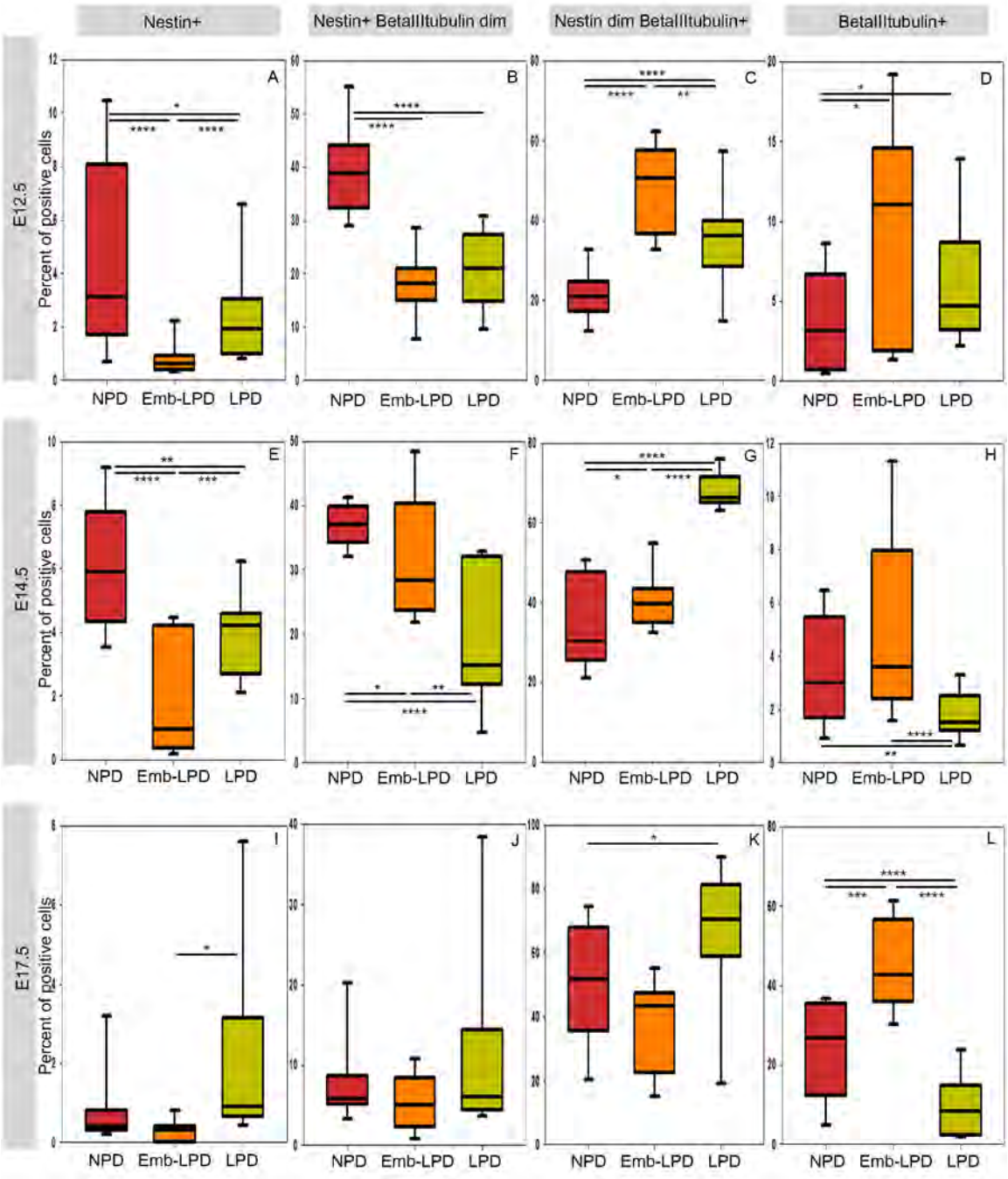

Fig. S2. Maternal diet affects expression of neural stem cells and neuronal differentiation markers analyzed by flow cytometry in cortical cells.
Quantification by flow cytometry of E12.5 (A-D) E14.5 (E-H) and E17.5 (I-L) cortical cells stained for Nestin and Beta-III-tubulin.
Nestin only positive cells (A,E,I), double positive cells separated into Nestin+ Beta-III-tubulin dim (B,F,J), and Nestin dim Beta-III-tubulin+ (C,G,K), and Beta-III-tubulin only positive cells (D,H,L) were quantified.
E12.5 cortex data represent n=24 (NPD), 18 (Emb-LPD), 21 (LPD) fetuses from 8 (NPD), 6 (Emb-LPD) or 7 (LPD) mothers.

E14.5 cortex data represent n=18 (NPD), 18 (Emb-LPD), 19 (LPD) fetuses from 6 (NPD), 6 (Emb-LPD) or 6 (LPD) mothers.
E17.5 cortex data represent n=18 (NPD), 18 (Emb-LPD), 18 (LPD) fetuses from 6 (NPD), 6 (Emb-LPD) or 6 (LPD) mothers.
Boxes represent interquartile ranges with middle lines representing the medians, whiskers (error bars) above and below the box indicate the 90th and 10th percentiles. *$p<0.05$, **$p<0.01$, ***$p<0.001$, ****$p<0.0001$.

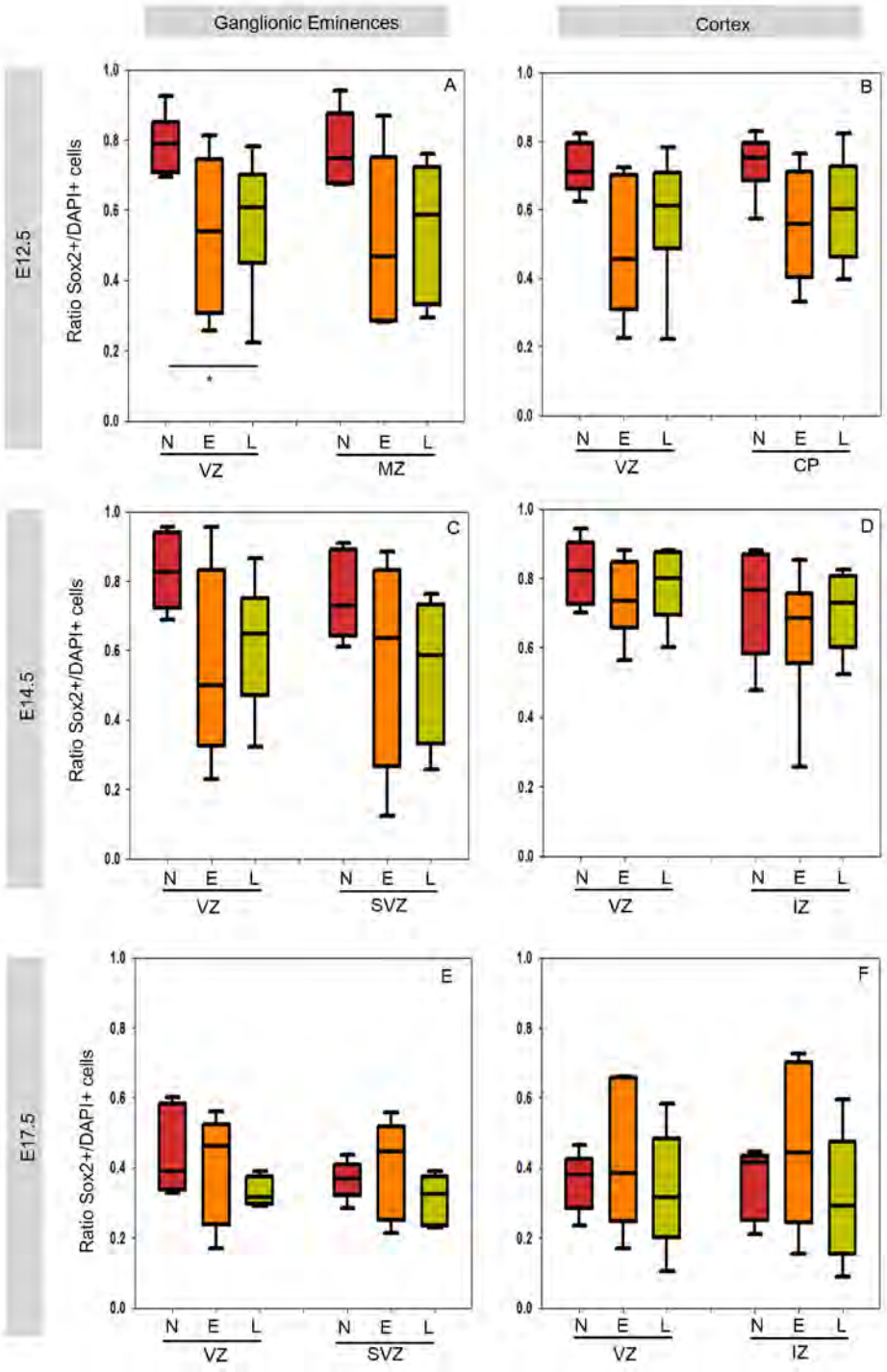

Fig. S3. Maternal diet affects regional expression of neural stem cells marker Sox2 analyzed by immunohistochemistry in ganglionic eminences and cortex.
Quantification of Sox2 staining (ratio of Sox2+/DAPI+ cells) on E12.5 ganglionic eminence (A) and cortex (B), on E14.5 ganglionic eminences (C) and cortex (D) and on E17.5 ganglionic eminences (E) and cortex (F) sections from different maternal diets.

Data represent 3 quantifications/layer/section of 3 sections/brain from 6 fetal brains from 6 different mothers per diet (E12.5 and E14.5) or from 5 fetal brains from 5 different mothers per diet (E17.5).
Boxes represent interquartile ranges with middle lines representing the medians, whiskers (error bars) above and below the box indicate the 90th and 10th percentiles. *p<0.05, **p<0.01, ***p<0.001, ****p<0.0001
N=NPD ; E=Emb=LPD ; L=LPD ; VZ=Ventricular Zone ; SVZ=Subventricular Zone; MZ=Mantle Zone ; IZ=Intermediate Zone ; CP=Cortical Plate.

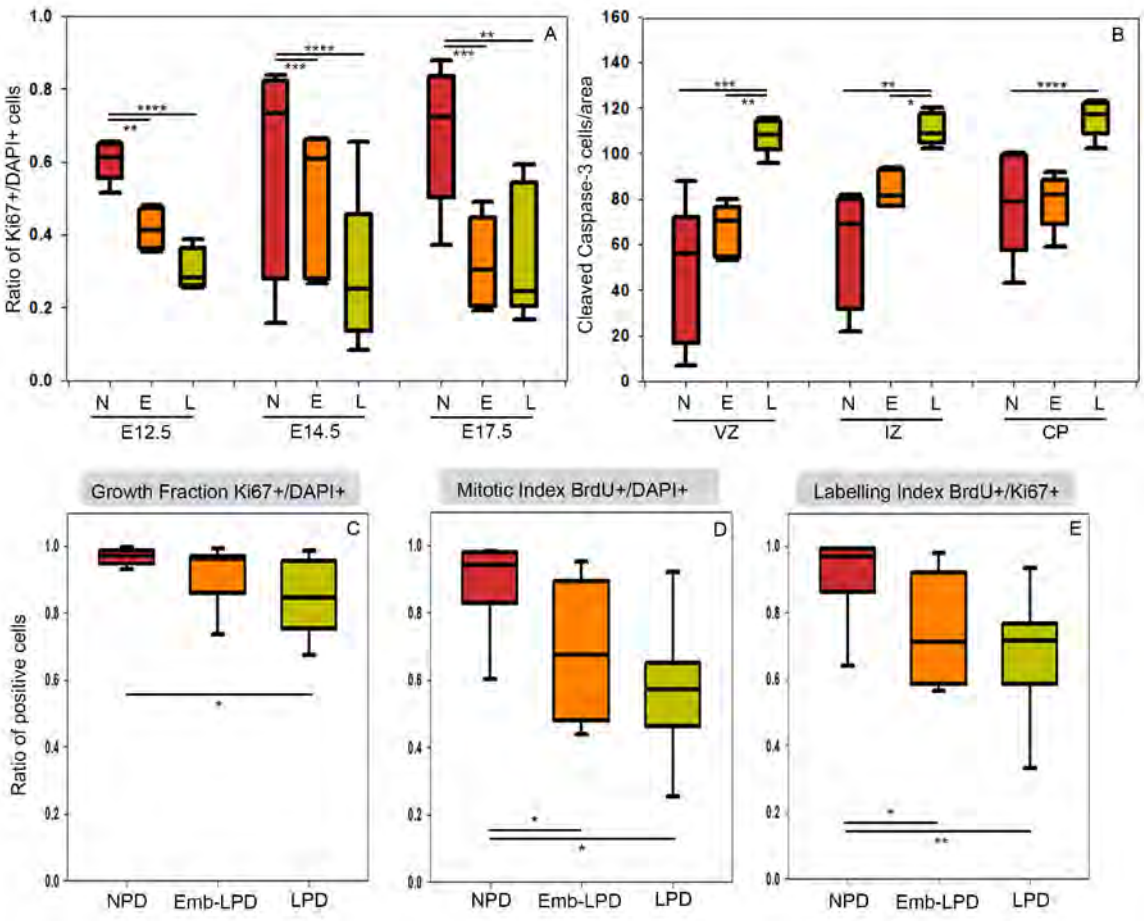

Fig. S4. Maternal diet affects proliferation and apoptosis in cortex and ganglionic eminences.
(A) The growth fraction quantifies the proportion of cells (DAPI+) which are proliferating (Ki67+) in E12.5, E14.5 and E17.5 cortical ventricular zone sections. Data represent 3 quantifications/layer/ section of 3 sections/brain from 5 fetal brains from 5 different mothers per diet.
(B) Quantification of Cleaved Caspase-3 staining (number of positive cells/area) on E17.5 cortical sections. Data represent 3 quantifications/layer/ section of 3 sections/brain from 5 fetal brains from 5 different mothers per diet.
Proliferation capacity was also analyzed *in vitro* by measuring proliferation indices (C,D,E) at day 3 of culture of E14.5 ganglionic eminences primary cells with n=8 (NPD), 7 (Emb-LPD), 8 (LPD) fetuses from 4 (NPD), 4(Emb-LPD) or 4 (LPD) mothers..
(C) The *in vitro* growth fraction quantifies the proportion of cells (DAPI+) which are proliferating (Ki67+).
(D) The *in vitro* mitotic index quantifies the proportion of cells (DAPI+) which are in S phase (BrdU+).
(E) The *in vitro* labeling index quantifies the proportion of proliferating cells (Ki67+) which are in S-phase (BrdU+).
Boxes represent interquartile ranges with middle lines representing the medians, whiskers (error bars) above and below the box indicate the 90th and 10th percentiles. *p<0.05, **p<0.01, ***p<0.001, ****p<0.0001. N=NPD; E=Emb=LPD; L=LPD; VZ=Ventricular Zone; SVZ=Subventricular Zone; MZ=Mantle Zone